An improved dissipative particle dynamics scheme

N. Mai-Duy[a,*], N. Phan-Thien[b] and T. Tran-Cong[a]
[a]Computational Engineering and Science Research Centre,
School of Mechanical and Electrical Engineering,
University of Southern Queensland, Toowoomba, QLD 4350, Australia
[b] Department of Mechanical Engineering, Faculty of Engineering,
National University of Singapore, 9 Engineering Drive 1, 117575, Singapore

Submitted to Applied Mathematical Modelling, Oct/2016; revised Jan/2017

ABSTRACT: Dissipative particle dynamics (DPD) and smoothed dissipative particle dynamics (sDPD) have become most popular numerical techniques for simulating mesoscopic flow phenomena in fluid systems. Several DPD/sDPD simulations in the literature indicate that the model fluids should be designed with their dynamic response, measured by the Schmidt number, in a relevant range in order to reach a good agreement with the experimental results. In this paper, we propose a new dissipative weighting function (or a new kernel) for the DPD (or the sDPD) formulation, which allows both the viscosity and the Schmidt number to be independently specified as input parameters. We also show that some existing dissipative functions/kernels are special cases of the proposed one, and the imposed viscosity of the present DPD/sDPD system has a lower and upper limit. Numerical verification of the proposed function/kernel is conducted in viscometric flows.

Keywords: Dissipative particle dynamics, kinetic theory, weighting functions, kernel functions, Schmidt number, mesoscale fluid systems.

1 Introduction

Dissipative particle dynamics (DPD) was introduced in 1992 by Hoogerbrugge and Koelman [1] as a coarse graining of molecular dynamics, intended for modelling complex fluids on a mesoscopic length scale. In DPD, the fluid, and everything in it, is represented by a set of particles (called DPD particles) that are free to move in space, each is supposed to represent a group of (molecular) particles. The motions of these DPD particles are governed by Newton's second law, where the forces acting on each particle consist of a conservative, a dissipative and a random forces. These forces drop off to zero outside a cut-off radius (which may be different for different types of forces). The conservative force is employed to provide a means to control the compressibility of the model fluid independently of the number density n, the cut-off radius r_c and the equilibrium temperature k_BT (mean specific kinetic energy) [2].

*Corresponding author E-mail: nam.mai-duy@usq.edu.au, Telephone +61-7-46312748, Fax +61-7-46312529

The dissipative force models viscous actions or hydrodynamic behaviour, which slows down the particles and thus to extract the system energy. The random force injects the kinetic energy to the DPD system to compensate for the lost energy due to dissipation. Later on, the DPD system is enforced to satisfy a thermal equilibrium according to a fluctuation-dissipation theorem (sometimes called detailed balance), resulting in some constraints on the dissipative and random forces [3]. All the DPD forces are pairwise, and are centre to centre. It should be pointed out that the DPD system conserves mass and momentum, both linear and angular, whilst maintains a constant temperature (specific kinetic energy) [4]. The DPD equations are stochastic equations that can be re-cast into a differential form by treating the random forces as a Wiener process. The numerical results over a large number of time steps are then averaged in small fixed collection bins to produce local density and local momentum. One can compute the stress tensor by means of Irving-Kirkwood formulation [5], which arises also from the conservation of linear momentum. Furthermore, the method possesses a free-scale property: a DPD system can be scaled so that one deals with a smaller number of particles; different levels of coarse graining with an appropriate scaling lead to the same calculated results [6]. It is noted that the link between the DPD and physical units is still not clear and further studies are needed. DPD can be understood as a bottom-up approach for handling complex fluids on mesoscopic length scale; the complex nature of the fluid is prescribed by the interaction between a subset of DPD particles (for example, chains as representative of polymers in a solution), e.g., [7,8,9].

On the other hand, the smoothed DPD method (sDPD) is a top-down approach for dealing with mesoscopic problems, derived directly from the Navier-Stokes equation with the inclusion of thermal fluctuation, where the random force is introduced in a way that satisfies a fluctuation-dissipation theorem [10]. Any non-Newtonian character of the fluid is explicitly specified in the constitutive equation, which is included in the Navier-Stokes equation. It can be seen that the formulations of DPD and sDPD have similar structures as they all involve conservative, dissipative and random forces. However, sDPD allows the viscosity (in fact, the whole rheology of the fluid via its constitutive equation) to be specified and the equation of state (pressure-density) as inputs of the simulation.

DPD and sDPD have been applied to various fluid dynamics problems; however, a complex structure fluid is not always modelled in the same way by the two versions. For example, in simulating particulate suspensions with DPD, a rigid particle can be represented effectively with only one DPD particle (the single particle model) [11], or by a few DPD particles (the spring model) [12,13], improving efficiency of the DPD simulation. To date, with sDPD, suspended particles have been modelled by the frozen particles [14] and thus a very much larger number of particles are required for a given volume fraction.

The dynamic response of a fluid can be measured by its Schmidt number, defined as the ratio of the the speed of momentum transfer (viscosity) to that of particles' diffusion (diffusivity)

$$S_c = \frac{\eta}{\rho D}, \tag{1}$$

where ρ is the fluid density, η is its viscosity, and D, its diffusivity. For sDPD, in principle, S_c can be arbitrarily large. However, simulations at large values of S_c using the standard predictor-corrector and velocity-Verlet schemes face a serious time-step limitation. Increasing the time-step size to a realistic value requires a splitting scheme [15]. For DPD, with the "standard" values of the input parameters, it has been shown that S_c is $O(1)$, which is much lower than that of a typical water-like liquid (e.g., for water, $S_c \sim 400$) [9]. As a result, special attention is needed in any simulation as the DPD system may not be in the correct regime of dynamic behaviour [16], for instance, in simulating dilute polymeric systems, it was found

that the Schmidt number of the solvent strongly affects nonequilibrium polymeric quantities [17]. Several studies [17,15] indicated that the model fluid should be designed with S_c in the relevant range in order to reach a good agreement with the experimental results. One can improve S_c by increasing the strength of the dissipative force, which requires a smaller time step to maintain temperature control, or simply modifying the standard weighting function for the dissipative force [18]. Analytic expressions for the self-diffusion coefficient have been derived from the kinetic theory for DPD [9,19,2] and from the equation of motion of a single particle for sDPD [20], where the conservative force is neglected in both cases. In both DPD and sDPD, the Schmidt number is a result of the choice of the parameters adopted, it has never been considered before as an input parameter.

In this study, we present some kinetic theory analysis for sDPD, introduce a new dissipative weighting function (or a new kernel) into the DPD (or the sDPD) equations which allows both the viscosity and the Schmidt number of the model fluids to be controlled, and compare the numerical performance in simulating viscometric flows between the proposed DPD (i.e., new dissipative weighting function, repulsion force derived from a soft potential form) and the proposed sDPD (new kernel, repulsion force derived from the discretisation of the pressure gradient term in the Navier-Stokes equation).

2 sDPD and DPD formulations

We briefly recall the isothermal Navier-Stokes equation for a compressible Newtonian fluid of density ρ, dynamic viscosity η_0 and volumetric viscosity ζ

$$\frac{d\rho}{dt} = -\rho\nabla.\mathbf{v}, \tag{2}$$

$$\rho\frac{d\mathbf{v}}{dt} = -\nabla P + \eta_0\nabla^2\mathbf{v} + \left(\zeta + \frac{\eta_0}{3}\right)\nabla\nabla.\mathbf{v}, \tag{3}$$

where t is the time, $\mathbf{v}$ the flow velocity and P the pressure.

Smoothed particle hydrodynamics (SPH) interpolations of some of the gradient terms that arise in the Navier-Stokes equation result in [10]

$$\frac{(\nabla P)_i}{d_i} = -\sum_j \left(\frac{P_i}{d_i^2} + \frac{P_j}{d_j^2}\right) F_{ij}\mathbf{r}_{ij}, \tag{4}$$

$$\frac{1}{d_i}\left(\nabla^2\mathbf{v}\right)_i = -2\sum_j \frac{F_{ij}}{d_i d_j}\mathbf{v}_{ij}, \tag{5}$$

$$\frac{1}{d_i}\left(\nabla\nabla.\mathbf{v}\right)_i = -\sum_j \frac{F_{ij}}{d_i d_j}\left[(\mathcal{D}+2)\mathbf{e}_{ij}\mathbf{e}_{ij}.\mathbf{v}_{ij} - \mathbf{v}_{ij}\right], \tag{6}$$

where $\mathcal{D}$ is the number of dimensions, $d_i(=1/V_i)$ is the number density of particle i (V_i is the volume of particle i), $\mathbf{e}_{ij} = \mathbf{r}_{ij}/r_{ij}$ a unit vector from particle j to particle i ($\mathbf{r}$ the position vector, $\mathbf{r}_{ij} = \mathbf{r}_i - \mathbf{r}_j$, $r_{ij} = |\mathbf{r}_{ij}|$), $\mathbf{v}_{ij} = \mathbf{v}_i - \mathbf{v}_j$ the relative velocity vector, and $F_{ij} = -W'(r_{ij}, h)/r_{ij}$ with h being the smoothing length of the kernel W which has two properties: (i) $[W]_R = 1$ and (ii) in the limit $h \to 0$, $W(r)$ tends to the Dirac function $\delta(r)$. Here we have employed the notation

$$[W]_R = \int d\mathbf{R}W(R). \tag{7}$$

Popular kernels in SPH include Lucy and quintic spline functions which are considered in this work.

If incompressibility of the fluid is invoked in the SPH discretisation, i.e., $(\nabla\nabla.\mathbf{v})_i = 0$, equation (6) leads to [21]

$$\mathbf{v}_{ij} = (\mathcal{D}+2)\mathbf{e}_{ij}\mathbf{e}_{ij}.\mathbf{v}_{ij}. \tag{8}$$

This gives rise to a SPH approximation of the incompressible isothermal Newtonian N-S equations as

$$m\frac{d\mathbf{v}_i}{dt} = \sum_j \left(\frac{P_i}{d_i^2} + \frac{P_j}{d_j^2}\right) r_{ij}F_{ij}\mathbf{e}_{ij} - 2\eta_0 \sum_j \frac{F_{ij}}{d_i d_j}\mathbf{v}_{ij}, \tag{9}$$

$$P_i = P_0\left[\left(\frac{\rho_i}{\rho_0}\right)^7 - 1\right], \quad \rho_i = md_i, \tag{10}$$

where P_0 is chosen in a way which results in a large speed of sound that can keep a relative density fluctuation small [22]. In this study, the relative density fluctuation is chosen less than 1% level, and consequently we choose $P_0 = c_s^2\rho_0/7$ (c_s is the speed of sound and ρ_0 the equilibrium (reference) density).

Substitution of (8), from the incompressibility constraint, into (9) yields

$$m\frac{d\mathbf{v}_i}{dt} = \sum_j \left(\frac{P_i}{d_i^2} + \frac{P_j}{d_j^2}\right) r_{ij}F_{ij}\mathbf{e}_{ij} - 2(\mathcal{D}+2)\eta_0 \sum_j \frac{F_{ij}}{d_i d_j}\mathbf{e}_{ij}\mathbf{e}_{ij}.\mathbf{v}_{ij}. \tag{11}$$

On a mesoscopic length scale, a fluctuation term is introduced into equation (11) (i.e., a smoothed DPD version) resulting in [10]

$$m\frac{d\mathbf{v}_i}{dt} = \sum_j \left(\frac{P_i}{d_i^2} + \frac{P_j}{d_j^2}\right) r_{ij}F_{ij}\mathbf{e}_{ij} - 2(\mathcal{D}+2)\eta_0 \sum_j \frac{F_{ij}}{d_i d_j}\mathbf{e}_{ij}\mathbf{e}_{ij}.\mathbf{v}_{ij} + \sqrt{2k_BT2(\mathcal{D}+2)\eta_0 \sum_j \frac{F_{ij}}{d_i d_j}}\theta_{ij}\mathbf{e}_{ij}, \tag{12}$$

where k_BT is the equilibrium temperature and θ_{ij} is a Gaussian white noise.

Returning to the DPD method, the fluid is replaced by a system of DPD particles undergoing their Newton's second law motion:

$$m\frac{d\mathbf{v}_i}{dt} = \sum_j \left(\mathbf{F}_{ij,C} + \mathbf{F}_{ij,D} + \mathbf{F}_{ij,R}\right), \tag{13}$$

where m and $\mathbf{v}_i$ represent the mass and velocity vector of a particle i, and the three forces on the right hand side represent the conservative force (subscript C), the dissipative force (subscript D) and the random force (subscript R):

$$\mathbf{F}_{ij,C} = a_{ij}w_C\mathbf{e}_{ij}, \tag{14}$$

$$\mathbf{F}_{ij,D} = -\gamma w_D\left(\mathbf{e}_{ij}\cdot\mathbf{v}_{ij}\right)\mathbf{e}_{ij}, \tag{15}$$

$$\mathbf{F}_{ij,R} = \sigma w_R\theta_{ij}\mathbf{e}_{ij}, \quad \sigma = \sqrt{2\gamma k_BT}, \tag{16}$$

where a_{ij}, γ and σ are constants reflecting the strengths of these forces, w_C, w_D and w_R the configuration-dependent weighting functions, and θ_{ij} a Gaussian white noise. It is noted

that $w_D(r)$ and $w_R(r)$ are dimensionless functions, γ has the unit of $[FT/L]$ and σ has the unit of $[F\sqrt{T}]$ ($[F]$, $[T]$ and $[L]$ are the unit of force, time and length, respectively). For w_C, there are several formes proposed, including purely repulsive, attractive-repulsive and multibody. In the present work, only the original (purely repulsive) form, which has been widely regarded as standard form, is considered. Hereafter, a DPD fluid is referred to as the model fluid corresponding to the purely repulsive form of the conservative force.

Drawing a comparison between (12) and (13), one may identify the different sDPD to DPD forces

$$a_{ij}w_C(r_{ij}) = \left(\frac{P_i}{d_i^2} + \frac{P_j}{d_j^2}\right) r_{ij}F_{ij}, \tag{17}$$

$$\gamma w_D(r_{ij}) = 2(\mathcal{D}+2)\eta_0 \frac{F_{ij}}{d_i d_j}, \tag{18}$$

$$\sigma w_R(r_{ij}) = \sqrt{2k_BT2(\mathcal{D}+2)\eta_0 \frac{F_{ij}}{d_i d_j}}, \tag{19}$$

or

$$a_{ij}w_C(r_{ij}) = \left(\frac{P_i}{d_i^2} + \frac{P_j}{d_j^2}\right) r_{ij}F_{ij}, \tag{20}$$

$$\gamma = 2(\mathcal{D}+2)r_c\eta_0, \quad w_D(r_{ij}) = \frac{F_{ij}}{r_c d_i d_j}, \tag{21}$$

$$\sigma = \sqrt{2k_BT2(\mathcal{D}+2)r_c\eta_0}, \quad w_R(r_{ij}) = \sqrt{\frac{F_{ij}}{r_c d_i d_j}}. \tag{22}$$

In both cases, DPD and sDPD, the random force is introduced in a way that satisfies a fluctuation-dissipation theorem.

3 Kinetic theory analysis

The sDDP equation (12) is rewritten in the form of standard DPD ((20)-(22)) and one can thus apply the kinetic theory results in DPD in its analysis [19,2].

In the absence of the conservative force ($\mathbf{F}_C(r) = 0$), using the kinetic theory, the expressions for the viscosity and diffusivity have been derived as [19,2]

$$\overline{\eta} = \frac{3mk_BT}{2\gamma[w_D]_R} + \frac{\gamma n^2[R^2 w_D]_R}{30}, \tag{23}$$

$$\overline{D} = \frac{3k_BT}{n\gamma[w_D]_R}, \tag{24}$$

where n is the number density, $[w_D]_R = \int d\mathbf{R} w_D(R)$ and $[R^2 w_D]_R = \int d\mathbf{R} R^2 w_D(R)$. In (23), there are two contributions to the viscosity $\overline{\eta}$, a kinetic part ($\overline{\eta}_K$) due to the motion of the individual particles (first term on RHS, called the "gas" contribution) and a dissipative part ($\overline{\eta}_D$) by the energy dissipation between particles (second term, called the "liquid" contribution). It is noted that, unlike the standard DPD, there are some constraints on $w_D(r_{ij}) = F_{ij}/(r_c d_i d_j) = -(1/(r_c d_i d_j r_{ij}))(dW/dr_{ij})$ in sDPD (e.g., $[W]_R = 1$ and $\lim_{r_c \to 0} W(r) = \delta(r)$).

In the case of Lucy function, function $F(r)$ takes the form

$$F(r) = -\frac{1}{r}\frac{dW}{dr} = \frac{315}{4\pi r_c^5}\left(1 - \frac{r}{r_c}\right)^2, \tag{25}$$

where the cut-off radius of the dissipative force (r_c) is taken as the smoothing length of the kernel h. Here, we assume that DPD particles have constant number density (i.e., $d_i = d_j = n$). For 3D space, we have $\gamma = 2(D+2)r_c\eta_0 = 10r_c\eta_0$ and

$$w_D(r) = \frac{F(r)}{n^2 r_c} = \frac{315}{4\pi n^2 r_c^6}\left(1 - \frac{r}{r_c}\right)^2. \tag{26}$$

Some simple integrations can be carried out to yield

$$[w_D]_R = \int d\mathbf{R} w_D(R) = \frac{315}{4\pi n^2 r_c^6} 4\pi r_c^3 \frac{1}{30} = \frac{21}{2}\frac{1}{n^2 r_c^3}, \tag{27}$$

$$[R^2 w_D(R)] = \int d\mathbf{R} R^2 w_D(R) = \frac{315}{4\pi n^2 r_c^6} 4\pi r_c^5 \frac{1}{105} = 3\frac{1}{n^2 r_c}. \tag{28}$$

The viscosity (23) reduces to

$$\overline{\eta} = \overline{\eta}_K + \overline{\eta}_D = \frac{1}{70}\frac{m k_B T n^2 r_c^2}{\eta_0} + \eta_0. \tag{29}$$

The possibility of using (29) as a mean to specify an arbitrary viscosity is noted. Expression (29) can be rearranged in the quadratic equation form for the specified input viscosity η_0

$$\eta_0^2 - \overline{\eta}\eta_0 + B = 0, \quad B = \frac{1}{70} m k_B T n^2 r_c^2. \tag{30}$$

For this to have a physical solution, we require

$$\overline{\eta}^2 \geq 4B = \frac{4}{70} m k_B T n^2 r_c^2. \tag{31}$$

For example, if $m = 1, k_B T = 1$ and $n = 4$, then $\overline{\eta} \geq 0.9562$ for $r_c = 1$ and $\overline{\eta} \geq 2.3905$ for $r_c = 2.5$. Suppose that this requirement is met, then the input viscosity can either be

$$\eta_0 = \frac{1}{2}\overline{\eta} + \frac{1}{2}\sqrt{\overline{\eta}^2 - 4B} \quad \text{or} \quad \eta_0 = \frac{1}{2}\overline{\eta} - \frac{1}{2}\sqrt{\overline{\eta}^2 - 4B}. \tag{32}$$

Since the first solution in (32) is the dissipative part of $\overline{\eta}$ and the second one the kinetic part of $\overline{\eta}$, only the first solution needs be considered if the viscosity for liquid is desired.

The self-diffusion coefficient (24) reduces to

$$\overline{D} = \frac{2\overline{\eta}_K}{mn} = \frac{1}{35}\frac{k_B T n r_c^2}{\eta_0}. \tag{33}$$

Consequently, the Schmidt number is

$$\overline{S}_c = \frac{\overline{\eta}}{\rho \overline{D}} = \frac{35\eta_0\overline{\eta}}{m k_B T n^2 r_c^2}. \tag{34}$$

Substitution of (33) into (34) yields $\overline{S}_c = \overline{\eta}/2\overline{\eta}_K$. At low Schmidt numbers, the kinetic part of the viscosity thus becomes noticeable. For such $\overline{S}_c$ values (some gas regime flow), as shown in Figure 1, the viscosity of the sDPD system $\overline{\eta}$ can be significantly different from the specified viscosity $\eta_0 = 1$ with increasing r_c.

Consider a generic tagged particle in a sea of other particles undergoing a diffusion process. According to the Stokes-Einstein relation, the size of a tagged particle (exclusion zone) can be estimated as

$$a_{eff} = \frac{k_B T}{6\pi \overline{D}\overline{\eta}}. \tag{35}$$

Substitution of (33) into (35) yields

$$a_{eff} = \frac{35\eta_0}{6\pi n r_c^2 \overline{\eta}}. \tag{36}$$

In the case of quintic spline function, using the same derivation procedure, expressions for the viscosity, self-diffusion coefficient, Schmidt number, and the size of a tagged particle are respectively given by

$$\overline{\eta} = \frac{1}{120}\frac{m k_B T n^2 r_c^2}{\eta_0} + \eta_0, \tag{37}$$

$$\overline{D} = \frac{1}{60}\frac{k_B T n r_c^2}{\eta_0}, \tag{38}$$

$$\overline{S}_c = \frac{60\eta_0\overline{\eta}}{m k_B T n^2 r_c^2}, \tag{39}$$

$$a_{eff} = \frac{10\eta_0}{6\pi n r_c^2 \overline{\eta}}. \tag{40}$$

4 Proposed dissipative weighting function/kernel

We propose a kernel that allows one to control both the viscosity and the Schmidt number of the sDPD fluid. The former is achieved by designing the proposed kernel to satisfy the properties of function W in SPH. The latter is achieved by introducing a free parameter, namely s, into the kernel. In other words, from a DPD perspective, there will be 2 free parameters (γ and s) in the dissipative force form and they are used to match the two dynamic thermo-properties, namely η and S_c, of a given fluid. Details are as follows.

4.1 Three dimensional space

To achieve the goals just mentioned, a kernel should be designed (i) to satisfy the properties of function W in SPH; and (ii) to result in function $F(r)$ in the form of $(1 - r/r_c)^s$. The kernel can be verified to be

$$W(r, r_c) = \frac{(s+3)(s+4)(s+5)}{32\pi r_c^3}\left(1 - \frac{r}{r_c}\right)^{s+1}\left[1 + (1+s)\frac{r}{r_c}\right], \quad s > 0, \tag{41}$$

where s is a free parameter. It has the same properties as SPH kernels (i.e., $[W]_R = 1$ and $\lim_{r_c \to 0} W(r, r_c) = \delta(r)$). It is noted that when $s = 2$, the proposed kernel reduces to Lucy function. The corresponding function $F(r)$ is

$$F(r) = -\frac{1}{r}\frac{\partial W}{\partial r} = \frac{(s+1)(s+2)(s+3)(s+4)(s+5)}{32\pi r_c^5}\left(1 - \frac{r}{r_c}\right)^s. \tag{42}$$

From (42), the weighting function for the dissipative force is derived

$$w_D(r) = \frac{F(r)}{n^2 r_c} = \frac{(s+1)(s+2)(s+3)(s+4)(s+5)}{32\pi n^2 r_c^6}\left(1-\frac{r}{r_c}\right)^s. \tag{43}$$

When $s = 1/2$, the proposed weighting function reduces to the one reported in [18] which is widely employed in DPD. It can be shown that

$$[w_D]_R = \frac{(s+4)(s+5)}{4n^2 r_c^3}, \quad [R^2 w_D]_R = \frac{3}{n^2 r_c}. \tag{44}$$

Using the kinetic theory, the dynamic thermo-properties of the sDPD fluid are estimated as

$$\overline{\eta} = \overline{\eta}_K + \overline{\eta}_D = \frac{3mk_BT}{2\gamma[w_D]_R} + \frac{\gamma n^2 [R^2 w_D]_R}{30} = \frac{3}{5}\frac{mk_BTn^2r_c^2}{\eta_0(s+4)(s+5)} + \eta_0, \tag{45}$$

$$\overline{D} = \frac{2\overline{\eta}_K}{mn} = \frac{6}{5}\frac{k_BTnr_c^2}{\eta_0(s+4)(s+5)}, \tag{46}$$

$$\overline{S}_c = \frac{\overline{\eta}}{mn\overline{D}} = \frac{5}{6}\frac{\overline{\eta}\eta_0(s+4)(s+5)}{mk_BTn^2r_c^2}, \tag{47}$$

$$a_{eff} = \frac{k_BT}{6\pi\overline{D}\overline{\eta}} = \frac{5}{36}\frac{\eta_0(s+4)(s+5)}{\pi n r_c^2 \overline{\eta}}. \tag{48}$$

Some conditions on (45)-(47) are required to ensure that the equations have a physical solution. For given values of m, k_BT, n and r_c, the minimum value of the viscosity $\overline{\eta}$ can be estimated by considering (45) as an equation for η_0. Multiplying both sides of (45) with η_0 yields

$$\eta_0^2 - \overline{\eta}\eta_0 + B = 0, \quad B = \frac{3}{5}\frac{mk_BTn^2r_c^2}{(s+4)(s+5)}, \tag{49}$$

leading to

$$\overline{\eta} \geq \sqrt{4B} = \sqrt{\frac{12}{5}\frac{mk_BTn^2r_c^2}{(s+4)(s+5)}}. \tag{50}$$

For liquid regime ($\overline{\eta}_K \ll \overline{\eta}_D$),

$$\overline{\eta} \simeq \eta_0 \geq \sqrt{\frac{12}{5}\frac{mk_BTn^2r_c^2}{(s+4)(s+5)}}. \tag{51}$$

As mentioned earlier, the free parameter s is introduced to make S_c become an input parameter to the DPD equation. To achieve this, we consider (47) as an equation for the variable s

$$s^2 + 9s + 20 - C = 0, \quad C = \frac{6}{5}\frac{\overline{S}_c mk_BTn^2r_c^2}{\overline{\eta}\eta_0} \simeq \frac{6}{5}\frac{\overline{S}_c mk_BTn^2r_c^2}{\eta_0^2}. \tag{52}$$

This equation always has two solutions. Since $s > 0$, we choose the following solution

$$s = \frac{-9 + \sqrt{1+4C}}{2}. \tag{53}$$

If the Schmidt number is given, then the value of s can be estimated from (53) (note that (53) is obtained by considering (47) as an equation in the variable s). If so, S_c is included into the DPD equation and the S_c of the DPD system as predicted by the kinetic theory will be exactly equal to this specified value.

The condition $s > 0$ requires $C > 20$. It implies that, for a given Schmidt number, the input viscosity should be chosen in a way that satisfies

$$\eta_0 < \sqrt{\frac{3}{50}\overline{S}_c m k_B T n^2 r_c^2}, \tag{54}$$

and for a given η_0, it requires

$$\overline{S}_c > \frac{50}{3}\frac{\eta_0^2}{m k_B T n^2 r_c^2}. \tag{55}$$

4.2 Two dimensional space

In 2D, the proposed kernel takes the form

$$W(r, r_c) = \frac{(s+3)(s+4)}{6\pi r_c^2}\left(1 - \frac{r}{r_c}\right)^{s+1}\left[1 + (1+s)\frac{r}{r_c}\right], \quad s > 0, \tag{56}$$

Relevant functions and dynamic thermo-properties of the sDPD fluid derived from this kernel are

$$F(r) = -\frac{1}{r}\frac{\partial W}{\partial r} = \frac{(s+1)(s+2)(s+3)(s+4)}{6\pi r_c^4}\left(1 - \frac{r}{r_c}\right)^{s}, \tag{57}$$

$$w_D(r) = \frac{F(r)}{n^2 r_c} = \frac{(s+1)(s+2)(s+3)(s+4)}{6\pi n^2 r_c^5}\left(1 - \frac{r}{r_c}\right)^{s}, \tag{58}$$

$$[w_D]_R = \frac{(s+3)(s+4)}{3n^2 r_c^3}, \quad [R^2 w_D]_R = \frac{2}{n^2 r_c}, \tag{59}$$

$$\overline{\eta} = \overline{\eta}_K + \overline{\eta}_D = \frac{m k_B T}{\gamma [w_D]_R} + \frac{\gamma n^2 [R^2 w_D]_R}{16} = \frac{3}{8}\frac{m k_B T n^2 r_c^2}{\eta_0 (s+3)(s+4)} + \eta_0, \tag{60}$$

$$\overline{D} = \frac{2\overline{\eta}_K}{mn} = \frac{3}{4}\frac{k_B T n r_c^2}{\eta_0 (s+3)(s+4)}, \tag{61}$$

$$\overline{S}_c = \frac{\overline{\eta}}{mn\overline{D}} = \frac{4}{3}\frac{\overline{\eta}\eta_0 (s+3)(s+4)}{m k_B T n^2 r_c^2}. \tag{62}$$

As in the 3D case, there are the following limits. The input viscosity can be imposed up to the value

$$\eta_0 < \sqrt{\frac{1}{16}\overline{S}_c m k_B T n^2 r_c^2}. \tag{63}$$

The viscosity of the system and the input Schmidt number cannot be lower than

$$\overline{\eta} \simeq \eta_0 \geq \sqrt{\frac{3}{2}\frac{m k_B T n^2 r_c^2}{(s+3)(s+4)}} \quad \text{and} \quad \overline{S}_c > \frac{16\eta_0^2}{m k_B T n^2 r_c^2}. \tag{64}$$

The Schmidt number can be incorporated into the DPD equation through

$$s = \frac{-7 + \sqrt{1 + 4C}}{2}, \quad C = \frac{3}{4}\frac{\overline{S}_c m k_B T n^2 r_c^2}{\overline{\eta}\eta_0} \simeq \frac{3}{4}\frac{\overline{S}_c m k_B T n^2 r_c^2}{\eta_0^2}. \tag{65}$$

Figure 2 display several kernels used in this study (i.e., Lucy function, quintic spline function and proposed function) and their associated dissipative weighting functions. Kinetic theory expressions for the viscosity, diffusivity and Schmidt number are shown in Table 1. If one is interested in modelling a liquid with the specified input viscosity, the DPD system should be designed in a way that makes $\overline{\eta}_K/\overline{\eta}_D$ small. This can be achieved by reducing $k_B T, m, n, r_c$ and/or increasing η_0. By choosing large values of η_0, and standard values of $k_B T, m, r_c$ and n [9], the kinetic part of $\overline{\eta}$ can be negligible.

4.3 Proposed DPD and sDPD

In this study, the DPD and sDPD formulations are implemented with the proposed dissipative weighting function (43) (or (58)) and the proposed kernel (41) (or (56)), respectively. The viscosity and the Schmidt number become input parameters. For the sDPD scheme, the repulsion force is the SPH discretisation of the pressure gradient term in the Navier-Stokes equation. Since the SPH quadrature (discretising) error is estimated as $O(\Delta x/r_c)$ (Δx is a typical distance between particles), one normally needs to employ relatively large values of r_c and n. For the DPD scheme, the repulsion force is derived from a soft potential and the repulsion strength is chosen according to the water compressibility. It is regarded as a coarse-grained model that possesses a scale-free property (i.e., independent of number density), and one can employ relatively small values of n (i.e., high coarse-graining levels) and r_c (i.e., $r_c = 1$ is the standard value). Kinetic theory expressions (34), (47) and (62) show that the S_c number is inversely proportional to n and r_c^3. In this sense, the proposed DPD has the ability to model a fluid that has a faster dynamic response than the proposed sDPD for a given input viscosity. In addition, the computational effort of the former is significantly less than that of the latter as the DPD does not involve the task of computing the number density.

4.4 Proposed DPD and Standard DPD

It can be seen that by choosing appropriate values of η and S_c for the proposed DPD and of γ and s for the standard DPD, the equations for the two methods are identical. However, the ways the simulations are conducted by the proposed and standard DPD are different. In the standard DPD, the noise level σ is considered as an input parameter. Its value is usually chosen as a compromise between fast simulation and satisfaction of the specified thermal temperature. Groot and Warren [16] recommended $\sigma = 3$ and this value has been widely used in practice. The viscosity and self-diffusivity are subsequently estimated by the kinetic theory or through numerical simulation. Any change in r_c, n, k_BT and m results in a DPD fluid of different viscosity. In the proposed DPD, the repulsion force is also derived from a soft potential, but the viscosity and the Schmidt number are input parameters. It is noted that the present weighting function for the dissipative force can also be implemented in conjunction with other forms of the conservative force. Like the standard DPD, one also needs to specify values of n, r_c, m and k_BT, but these values can be designed so that their effects on the viscosity of the system can be negligible.

We now examine the ways to control other hydrodynamic properties (e.g., the self-diffusion coefficient and Schmidt number) of the DPD fluid by the two methods. The diffusivity in the standard DPD with $s = 1/2$ is estimated as [9]

$$\overline{D} = \frac{315}{32\pi}\frac{k_BT^2}{\sigma^2 n r_c^3}, \tag{66}$$

which shows that the self-diffusivity is inversely proportional to n and r_c^3. In contrast, from (46) and (61), the self-diffusivity is proportional to n and r_c for the proposed DPD. As the level of coarse-graining increases, the number density used is reduced, leading to a decrease in $\overline{D}$ and an increase in $\overline{S}_c$ for the proposed DPD, but an increase in $\overline{D}$ and a decrease in $\overline{S}_c$ for the standard DPD. In this regard, the proposed DPD is preferable to the standard DPD in the context of coarse grained modelling.

We recall the size of a particle in the standard DPD (with $s = 1/2$) produced by the dissipative force [13]

$$a_{eff} = \frac{56320\pi n\sigma^4 r_c^6}{315 \times 51975m(k_BT)^3 + 64 \times 256\pi^2\sigma^4 n^2 r_c^8}. \tag{67}$$

Together with (48), the effective size of a particle can be seen to be a decreasing function of r_c for both the standard DPD and the proposed DPD.

5 Numerical results

Verification of the proposed weighting function/kernel is conducted in no-flow condition and in viscometric flows. For the latter, we consider Couette flow with Lees-Edwards boundary conditions [23]. Simulations are carried out using 30,000 time steps and $\Delta t = 0.001$ for computing the diffusivity, and using 200,000 time steps and $\Delta t = 0.005$ to compute the viscosity. To assess the performance of different DPD formulations, a range of shear rate is employed, over which we measure the mean value and standard deviation of the computed viscosities. The standard deviation is expected to be small as the viscosity is constant for a Newtonian fluid.

5.1 Proposed function with $s = 1/2$

The proposed function/kernel is first implemented with $s = 1/2$ and the obtained results are compared with those by the sDPD using Lucy and quintic spline kernels. Note that $s = 1/2$ is widely employed in the standard DPD (e.g. [18]). The imposed viscosities are chosen to be $\eta_0 = 10$ and $\eta_0 = 50$. Since the value of s here is fixed, the Schmidt number is a result of the choice of the input parameters. According to the kinetic theory, the three kernels, Lucy, quintic and proposed, have $\overline{S}_c \sim O(10^2)$ and $\sim O(10^3)$ for $\eta_0 = 10$ and $\eta_0 = 50$, respectively.

Table 2 shows the numerical results obtained by the proposed DPD and sDPD methods using $(r_c = 2.5, m = 1, k_BT = 1, n = 4)$ for two input viscosities, namely 10 and 50. Results by the sDPD using Lucy and quintic kernels, where the conservation of angular momentum is guaranteed, are also included. The calculated viscosity is seen to be more stable with the proposed function ($s = 1/2$) than with Lucy ($s = 2$) and Quintic functions over the range of the imposed shear rate. Results concerning the standard deviation of the computed viscosities by the proposed sDPD are higher than those by the proposed DPD.

When r_c is reduced to 1, numerical experiments (Table 3) indicates that the sDPD fails to represent a fluid properly - its viscosity is erratic in the shear rate. In contrast, the proposed DPD produces a stable viscosity over a range of the imposed shear rate (0.05, 0.1, 0.2, 0.5, 1). For the sDPD, with $r_c = 1$ and $n = 4$, the discretisation appears too coarse for a proper simulation. For the proposed DPD, good results are obtained as the method is a coarse-grained model that is also free-scale. Furthermore, as shown in Figure 3, linear velocity profiles are obtained and the computed thermal temperature and number density are approximately equal to 1 and 4, respectively. Also, the shear stress is typically "constant" across the flow section and the normal stress difference is approximately zero.

5.2 Proposed function with s as a function of S_c

Taking $n = 4, k_BT = 1, r_c = 2.5$ and $m = 1$, through (63), the upper limit of the imposed viscosity is estimated as 50 for $S_c = 400$ and 79.1 for $S_c = 10^3$. Appropriate values of η_0 are then chosen, from which the corresponding values of the free parameter s are obtained. Results concerning the viscosity are presented in Table 4 for the proposed sDPD and in Table 5 for the proposed DPD. It can be seen that the exponent s is covered from a nearly-zero value to the value of about 2 (Lucy kernel has $s = 2$). Similar remarks to the case of $s = 1/2$, where S_c is a result of the choice of the parameters adopted (Section 5.1), can be made here. Note that the results tabulated in the tables here correspond to the specified S_c. The standard deviation of the computed viscosities is relatively small and the calculated viscosities are in good agreement with the imposed viscosity or the viscosity by the kinetic theory over a range of the shear rate. Furthermore, it can be seen that low values of s generally lead to more stable calculated results than large values of s for a given Sc. The reason for this is still not clear to the present authors. The differences between the mean computed viscosity and the viscosity by the kinetic theory are in the range of 0.4% to 3.6% for $S_{c0} = 400$, and of 0.7% to 4.2% for $S_{c0} = 1000$ for the proposed sDPD, and 0.8% to 4.1% for $S_{c0} = 400$, and 1.0% to 4.6% for $S_{c0} = 1000$ for the proposed DPD. These values are small in comparison to the error of the order $10 - 30\%$ by the standard DPD reported in [16].

No-flow simulations are also conducted to compute the diffusivity of the DPD/sDPD fluid for a wide range of the Schmidt number, namely $(10, 20, \cdots, 90, 100, 200, \cdots, 1000)$. The imposed viscosities are chosen near their upper limits. Variations of the mean squared displacement of the particles against time can be well approximated by polynomials of first order. Some typical results of the diffusivity are displayed in Figure 4. For $S_{c0} = 400$ and $\eta_0 = 49$, the self-diffusion coefficient is estimated as 0.0346 by the proposed sDPD and 0.0319 by the proposed DPD, which are comparable to the value of 0.0306 predicted by the kinetic theory.

Figure 5 displays the computed S_c against the imposed value S_{c0} in the log-scale coordinate system by the three methods. It can be seen that values of the Schmidt number predicted by the kinetic theory very much agree with the computed (and specified) values as expected; the formulation is doing its job well. The computed S_c values by the proposed sDPD and DPD are in good agreement with the kinetic theory predictions, particularly for the proposed DPD. It is noted that the error bars associated with the data points are not displayed here since their values are quite small in comparison with the coordinate scale used.

6 Concluding remarks

This paper presents improved DPD and sDPD formulations for simulating mesoscopic phenomena in fluid systems. A new dissipative weighting function/kernel is introduced into the DPD/sDPD formulation, which allows both the viscosity and the Schmidt number of the DPD/sDPD fluid to be specified as input parameters. Numerical results show that (i) calculated viscosities, self-diffusion coefficient and Schmidt numbers by the proposed schemes are in good agreement with those by the kinetic theory; and (ii) the proposed DPD scheme (i.e., new weighting function, repulsion force derived from a soft potential) is superior to the proposed sDPD scheme (new kernel, repulsion force derived from the pressure gradient

discretisation) in terms of computational effort and ability to yield a stable viscosity from different imposed shear rates.

References

1. P.J. Hoogerbrugge, J.M.V.A. Koelman, Simulating microscopic hydrodynamic phenomena with dissipative particle dynamics, Europhysics Letters. 19(3) (1992) 155-160.

2. C. Marsh, Theoretical aspect of dissipative particle dynamics (PhD Thesis), University of Oxford, 1998.

3. P. Español, P. Warren, Statistical mechanics of dissipative particle dynamics, Europhysics Letters. 30(4) (1995) 191-196.

4. P. Español, Hydrodynamics from dissipative particle dynamics, Phys. Rev. E. 52 (1995) 1734-1742.

5. J.H. Irving, J.G. Kirkwood, The statistical mechanical theory of transport processes. IV. The equations of hydrodynamics, J. Chem. Phys. 18 (1950) 817-829.

6. R.M. Füchslin, H. Fellermann, A. Eriksson, H.-J. Ziock, Coarse graining and scaling in dissipative particle dynamics, J. Chem. Phys. 130 (2009) 214102.

7. Y. Kong, C.W. Manke, W.G. Madden, A.G. Schlijper, Effect of solvent quality on the conformation and relaxation of polymers via dissipative particle dynamics, J. Chem. Phys. 107 (1997) 592.

8. E.S. Boek, P.V. Coveney, H.N.N. Lekkerkerker, P. van der Schoot, Simulating the rheology of dense colloidal suspensions using dissipative particle dynamics, Phys. Rev. E. 55(3) (1997) 3124-3133.

9. N. Phan-Thien, Understanding Viscoelasticity: An Introduction to Rheology, second Edition, Springer-Verlag, Berlin, 2013.

10. P. Español, M. Revenga, Smoothed dissipative particle dynamics, Phys. Rev. E. 67(2) (2003) 026705.

11. W. Pan, B. Caswell, G.E. Karniadakis, Rheology, microstructure and migration in Brownian colloidal suspensions, Langmuir. 26(1) (2010) 133-142.

12. N. Phan-Thien, N. Mai-Duy, B.C. Khoo, A spring model for suspended particles in dissipative particle dynamics, J. Rheol. 58 (2014) 839-867.

13. N. Mai-Duy, N. Phan-Thien, B.C. Khoo, Investigation of particles size effects in Dissipative Particle Dynamics (DPD) modelling of colloidal suspensions, Comput. Phys. Comm. 189 (2015) 37-46.

14. X. Bian, S. Litvinov, R. Qian, M. Ellero, N.A. Adams, Multiscale modeling of particle in suspension with smoothed dissipative particle dynamics, Phys. Fluids. 24 (2012) 012002.

15. S. Litvinov, M. Ellero, X.Y. Hu, N.A. Adams, A splitting scheme for highly dissipative smoothed particle dynamics, J. Comput. Phys. 229(15) (2010) 5457-5464.

16. R.D. Groot, P.B. Warren, Dissipative particle dynamics: Bridging the gap between atomistic and mesoscopic simulation, J. Chem. Phys. 107 (1997) 4423.

17. V. Symeonidis, G.E. Karniadakis, B. Caswell, Schmidt number effects in dissipative particle dynamics simulation of polymers, J. Chem. Phys. 125 (2006) 184902.

18. X.J. Fan, N. Phan-Thien, S. Chen, X. Wu, T.Y. Ng, Simulating flow of DNA suspension using dissipative particle dynamics, Phys. Fluids. 18(6) (2006) 063102.

19. C.A. Marsh, G. Backx, M.H. Ernst, Static and dynamic properties of dissipative particle dynamics, Phys. Rev. E. 56(2) (1997) 1676-1691.

20. S. Litvinov, M. Ellero, X. Hu, N.A. Adams, Self-diffusion coefficient in smoothed dissipative particle dynamics, J. Chem. Phys. 130 (2009) 021101.

21. X.Y. Hu, N.A. Adams, Angular-momentum conservative smoothed particle dynamics for incompressible viscous flows, Phys. Fluids. 18 (2006) 101702.

22. J.J. Monaghan, Smoothed particle hydrodynamics, Reports on Progress in Physics. 68(8) (2005) 1703.

23. A.W. Lees, S.F. Edwards, The computer study of transport processes under extreme conditions, Journal of Physics C: Solid State Physics. 5(15) (1972) 1921.

Table 1: Diffusivity, viscosity and Schmidt number predicted by kinetic theory for sDPD

Lucy	Quintic	Proposed ($s = 1/2$)
	$w_D(r),\ r \leq 1$	
$\sim (1-r)^2$	$\sim \begin{cases} (3-3r)^4 - 6\,(2-3r)^4 + 15\,(1-3r)^4 \\ (3-3r)^4 - 6\,(2-3r)^4 \\ (3-3r)^4 \end{cases}$	$\sim (1-r)^{1/2}$
	Dissipative viscosity, 2D & 3D	
η_0	η_0	η_0
	Kinetic viscosity, 2D	
$\frac{1}{80}\frac{mk_BTn^2r_c^2}{\eta_0}$	$\frac{239}{33264}\frac{mk_BTn^2r_c^2}{\eta_0}$	$\frac{1}{42}\frac{mk_BTn^2r_c^2}{\eta_0}$
	$100(\overline{\eta}_K/\eta_0)$ for $m=1, k_BT=1, n=4, r_c=1, \eta_0=10$	
0.20%	0.11%	0.38%
	Kinetic viscosity, 3D	
$\frac{1}{70}\frac{mk_BTn^2r_c^2}{\eta_0}$	$\frac{1}{120}\frac{mk_BTn^2r_c^2}{\eta_0}$	$\frac{4}{165}\frac{mk_BTn^2r_c^2}{\eta_0}$
	$100(\overline{\eta}_K/\eta_0)$ for $m=1, k_BT=1, n=4, r_c=1, \eta_0=10$	
0.22%	0.13%	0.38%
	Self-diffusion coefficient, 2D	
$\frac{1}{40}\frac{k_BTnr_c^2}{\eta_0}$	$\frac{239}{16632}\frac{k_BTnr_c^2}{\eta_0}$	$\frac{1}{21}\frac{k_BTnr_c^2}{\eta_0}$
	Self-diffusion coefficient, 3D	
$\frac{1}{35}\frac{k_BTnr_c^2}{\eta_0}$	$\frac{1}{60}\frac{k_BTnr_c^2}{\eta_0}$	$\frac{8}{165}\frac{k_BTnr_c^2}{\eta_0}$
	Schmidt number, 2D	
$\frac{40\eta_0(\overline{\eta}_K+\eta_0)}{mk_BTn^2r_c^2}$	$\frac{16632}{239}\frac{\eta_0(\overline{\eta}_K+\eta_0)}{mk_BTn^2r_c^2}$	$\frac{21\eta_0(\overline{\eta}_K+\eta_0)}{mk_BTn^2r_c^2}$
	Schmidt number, 3D	
$\frac{35\eta_0(\overline{\eta}_K+\eta_0)}{mk_BTn^2r_c^2}$	$\frac{60\eta_0(\overline{\eta}_K+\eta_0)}{mk_BTn^2r_c^2}$	$\frac{165}{8}\frac{\eta_0(\overline{\eta}_K+\eta_0)}{mk_BTn^2r_c^2}$

Table 2: Couette flow, $r_c = 2.5, m = 1, k_BT = 1, n = 4$: Variation in the computed viscosity $\overline{\eta}^*$ over a range of shear rate (0.05, 0.1, 0.2, 0.5, 1). Note that η_0 is the input viscosity, $\overline{\eta}$ the viscosity by the kinetic theory and $\overline{\eta}^*$ the viscosity obtained from numerical simulation, where the shear stress is calculated using the Irving-Kirkwood formula. The proposed function/kernel consistently outperforms the Lucy and quintic kernels. However, solutions by the proposed sDPD are still less stable than those by the proposed DPD.

	$\eta_0 = 10$							
Method	$\overline{\eta}$	$\overline{\eta}^*$					mean($\overline{\eta}^*$)	std($\overline{\eta}^*$)
sDPD (Lucy)	10.1250	8.9345	9.7711	9.9974	10.3299	10.5475	9.9161	0.6247
sDPD (quintic)	10.0718	8.7544	9.2305	9.6393	10.2517	10.6194	9.6991	0.7530
Proposed sDPD ($s = 1/2$)	10.2381	10.0224	9.9574	10.3460	10.6081	10.7689	10.3406	0.3547
Proposed DPD ($s = 1/2$)	10.2381	10.0457	10.0344	10.2302	10.1977	10.1982	10.1412	0.0934

	$\eta_0 = 50$							
Method	$\overline{\eta}$	$\overline{\eta}^*$					mean($\overline{\eta}^*$)	std($\overline{\eta}^*$)
sDPD (Lucy)	50.0250	45.3252	46.9274	48.1738	49.4448	50.1124	47.9967	1.9290
sDPD (quintic)	50.0144	41.7764	44.3180	46.5540	48.7942	49.9483	46.2782	3.3160
Proposed DPD ($s = 1/2$)	50.0476	48.0100	48.9023	49.6504	50.1365	50.5073	49.4413	1.0003
Proposed sDPD ($s = 1/2$)	50.0476	49.2684	49.3672	49.3490	49.2771	49.1392	49.2802	0.0899

Table 3: Couette flow, $r_c = 1, \eta_0 = 10, m = 1, k_B T = 1, n = 4$, 200000 time steps: Variation in the computed viscosity $\overline{\eta}^*$ over a range of shear rate (0.05, 0.1, 0.2, 0.5, 1). Note that η_0 is the input viscosity, $\overline{\eta}$ the viscosity by the kinetic theory and $\overline{\eta}^*$ the viscosity obtained from simulation, where the shear stress is calculated using the Irving-Kirkwood formula. With $r_c = 1$, the proposed DPD is able to produce reasonable (constant) values of viscosity, probably owing to the fact that DPD is a coarse-grained model. In contrast, the sDPD fails to represent a fluid properly as the SPH discretisation ($r_c = 1, n = 4$) used for the pressure gradient term appears too coarse.

Methood	η_0	$\overline{\eta}$	$\overline{\eta}^*$					mean($\overline{\eta}^*$)	std($\overline{\eta}^*$)
sDPD (Lucy)	10	10.0200	5.3589	6.7573	8.2504	10.4305	11.6631	8.4920	2.5835
Proposed DPD ($s = 1/2$)	10	10.0381	9.3215	9.3359	9.3162	9.3038	9.2621	9.3079	0.0281

Table 4: Couette flow, the proposed sDPD method with η and S_c as specified inputs, $r_c = 2.5, m = 1, k_BT = 1, n = 4$: Variation in the computed viscosity $\overline{\eta}^*$ over a range of shear rate (0.05, 0.1, 0.2, 0.5, 1). Note that η_0 is the input viscosity, $\overline{\eta}$ the viscosity by the kinetic theory and $\overline{\eta}^*$ the viscosity obtained from numerical simulation, where the shear stress is calculated using the Irving-Kirkwood formula. The differences between the mean computed viscosity and the viscosity by the kinetic theory are in the range of 0.4% to 3.6% for $S_{c0} = 400$, and of 0.7% to 4.2% for $S_{c0} = 1000$. These values are small in comparison to the error within $10 - 30\%$ by the standard DPD reported in [16].

S_{c0}	η_0	s	$\overline{\eta}$	$\overline{\eta}^*$					mean($\overline{\eta}^*$)	std($\overline{\eta}^*$)
400	49	0.0700	49.0613	47.7375	48.4364	48.8504	49.3434	49.7297	48.8195	0.7780
400	47	0.2190	47.0588	45.4489	46.2492	46.8671	47.2996	47.6171	46.6964	0.8656
400	45	0.3813	45.0562	43.3741	44.1802	44.7504	45.2320	45.5524	44.6178	0.8670
400	43	0.5589	43.0538	41.3130	42.0243	42.6415	43.1952	43.5018	42.5352	0.8854
400	41	0.7540	41.0513	39.1793	39.8760	40.5759	41.1509	41.3715	40.4307	0.9081
400	39	0.9692	39.0487	37.2602	37.8281	38.4795	39.1449	39.4477	38.4321	0.9055
400	37	1.2078	37.0463	34.7002	35.5805	36.3823	37.1015	37.4051	36.2339	1.1097
400	35	1.4739	35.0438	32.5375	33.4678	34.3204	34.9989	35.3611	34.1371	1.1490
400	33	1.7724	33.0412	30.3894	31.3612	32.1233	32.9044	32.9044	31.9365	1.0762
400	31	2.1096	31.0388	28.1541	29.1638	30.0406	30.8461	31.2780	29.8965	1.2653
10^3	79	0.0025	79.0395	76.6289	77.8186	78.6003	79.3046	79.7997	78.4304	1.2538
10^3	77	0.0916	77.0385	74.7041	75.8645	76.6242	77.2293	77.6836	76.4211	1.1775
10^3	75	0.1856	75.0375	72.7499	73.6112	74.4687	75.2163	75.5948	74.3282	1.1638
10^3	73	0.2847	73.0365	70.4257	71.6010	72.5202	73.1585	73.5223	72.2455	1.2516
10^3	71	0.3895	71.0355	68.5890	69.4303	70.3697	71.0520	71.4883	70.1859	1.1833
10^3	69	0.5004	69.0345	66.2309	67.2835	68.3294	68.9801	69.4448	68.0537	1.3024
10^3	67	0.6179	67.0335	64.0793	65.3608	66.1952	66.9552	67.3636	65.9908	1.3141
10^3	65	0.7428	65.0325	61.8990	63.2600	64.0791	64.8594	65.3057	63.8806	1.3546
10^3	63	0.8757	63.0315	59.8127	61.0272	61.9825	62.8354	63.3446	61.8005	1.4175
10^3	61	1.0173	61.0305	57.4479	59.0441	59.8442	60.8260	61.3698	59.7064	1.5475
10^3	59	1.1686	59.0295	55.2255	56.7873	57.7469	58.7908	59.2891	57.5679	1.6268
10^3	57	1.3305	57.0285	53.3352	54.4782	55.6355	56.7415	57.2036	55.4788	1.5961
10^3	55	1.5043	55.0275	50.9466	52.2703	53.6639	54.6674	55.1483	53.3393	1.7327
10^3	53	1.6913	53.0265	48.8375	50.2005	51.4116	52.5052	53.1137	51.2137	1.7313
10^3	51	1.8931	51.0255	46.4816	48.1016	49.3296	50.4452	51.1405	49.0997	1.8627
10^3	49	2.1113	49.0245	44.1459	45.9347	47.1279	48.4088	49.0649	46.9364	1.9701

Table 5: Couette flow, the proposed DPD method with η and S_c as specified inputs, $r_c = 2.5, m = 1, k_BT = 1, n = 4$, 200000 time steps: Variation in the computed viscosity $\overline{\eta}^*$ over a range of shear rate (0.05, 0.1, 0.2, 0.5, 1). Note that η_0 is the input viscosity, $\overline{\eta}$ the viscosity by the kinetic theory and $\overline{\eta}^*$ the viscosity obtained from numerical simulation, where the shear stress is calculated using the Irving-Kirkwood formula. The differences between the mean computed viscosity and the viscosity by the kinetic theory are in the range of 0.8% to 4.1% for $S_{c0} = 400$, and of 1.0% to 4.6% for $S_{c0} = 1000$. These values are small in comparison to the error within $10 - 30\%$ by the standard DPD reported in [16].

S_{c0}	η_0	s	$\overline{\eta}$	$\overline{\eta}^*$					mean($\overline{\eta}^*$)	std($\overline{\eta}^*$)
400	49	0.0700	49.0613	48.6527	48.6499	48.6072	48.5680	48.5020	48.5960	0.0630
400	47	0.2190	47.0588	46.5280	46.5480	46.5677	46.5308	46.4424	46.5234	0.0480
400	45	0.3813	45.0562	44.4845	44.5760	44.5253	44.4635	44.3705	44.4840	0.0766
400	43	0.5589	43.0538	42.4420	42.4700	42.5166	42.3820	42.2749	42.4171	0.0932
400	41	0.7540	41.0513	40.4706	40.3918	40.4173	40.3121	40.2135	40.3611	0.1003
400	39	0.9692	39.0487	38.3384	38.3526	38.3091	38.2067	38.1076	38.2629	0.1039
400	37	1.2078	37.0463	36.3077	36.3432	36.1828	36.1117	35.9647	36.1820	0.1533
400	35	1.4739	35.0438	34.1004	34.1354	34.1335	33.9547	33.8340	34.0316	0.1331
400	33	1.7724	33.0412	32.0159	31.9489	31.9399	31.7961	31.6702	31.8742	0.1394
400	31	2.1096	31.0388	29.8289	29.9010	29.8028	29.6245	29.4874	29.7289	0.1690
10^3	79	0.0025	79.0395	78.2694	78.3023	78.2876	78.1766	77.9877	78.2047	0.1308
10^3	77	0.0916	77.0385	76.3450	76.2902	76.3054	76.1304	75.9391	76.2020	0.1682
10^3	75	0.1856	75.0375	74.2632	74.3087	74.1706	74.0582	73.8520	74.1305	0.1829
10^3	73	0.2847	73.0365	72.2327	72.2330	72.1074	71.9916	71.7881	72.0706	0.1871
10^3	71	0.3895	71.0355	70.1473	70.1546	70.0979	69.9238	69.6816	70.0010	0.2015
10^3	69	0.5004	69.0345	67.9465	68.0606	68.0470	67.8259	67.6197	67.8999	0.1828
10^3	67	0.6179	67.0335	66.0183	66.0046	65.9752	65.7646	65.5433	65.8612	0.2053
10^3	65	0.7428	65.0325	63.9088	63.9030	63.8650	63.6619	63.4285	63.7534	0.2079
10^3	63	0.8757	63.0315	61.8891	61.9422	61.7653	61.5269	61.3271	61.6901	0.2585
10^3	61	1.0173	61.0305	59.9201	59.8296	59.6849	59.4454	59.2193	59.6199	0.2869
10^3	59	1.1686	59.0295	57.7898	57.8112	57.5797	57.3167	57.0336	57.5062	0.3310
10^3	57	1.3305	57.0285	55.6375	55.6135	55.4978	55.1821	54.8979	55.3658	0.3183
10^3	55	1.5043	55.0275	53.3698	53.5036	53.3964	53.0487	52.7674	53.2172	0.3034
10^3	53	1.6913	53.0265	51.4842	51.3216	51.1973	50.8794	50.5953	51.0956	0.3569
10^3	51	1.8931	51.0255	49.3580	49.1922	49.0333	48.7463	48.4186	48.9497	0.3728
10^3	49	2.1113	49.0245	47.0571	46.9792	46.8377	46.5509	46.2284	46.7307	0.3407

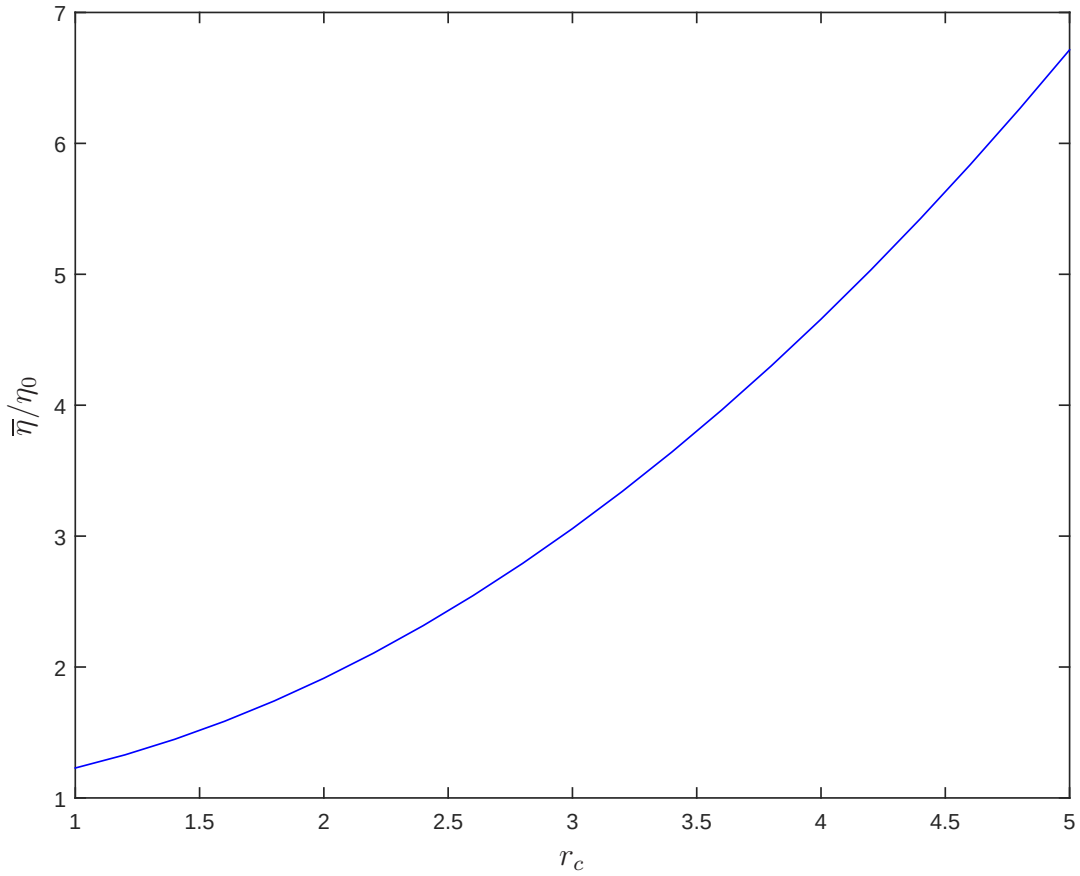

Figure 1: Kinetic theory, Lucy kernel, $m = 1, k_B T = 1, n = 4, \eta_0 = 1$, low Schmidt numbers (some gas regime): The difference between the viscosity of the sDPD system $\overline{\eta}$ and the imposed viscosity η_0 significantly increases with the cut-off radius r_c.

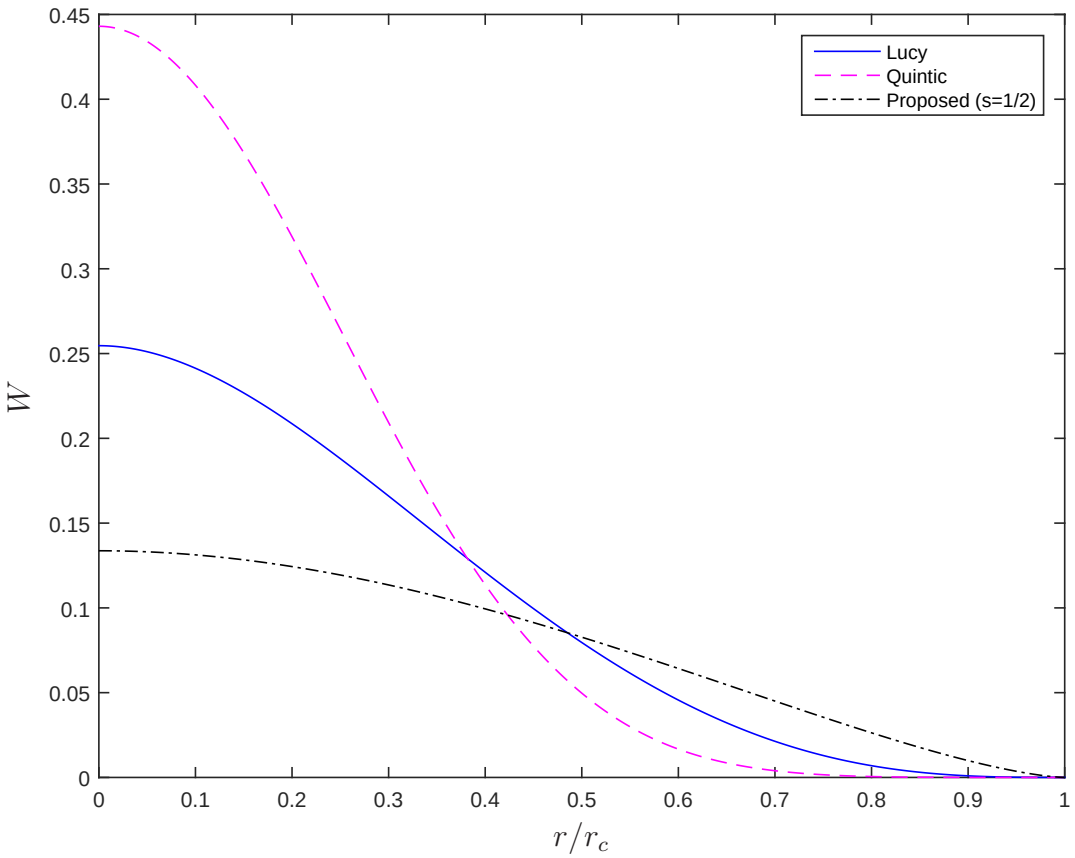

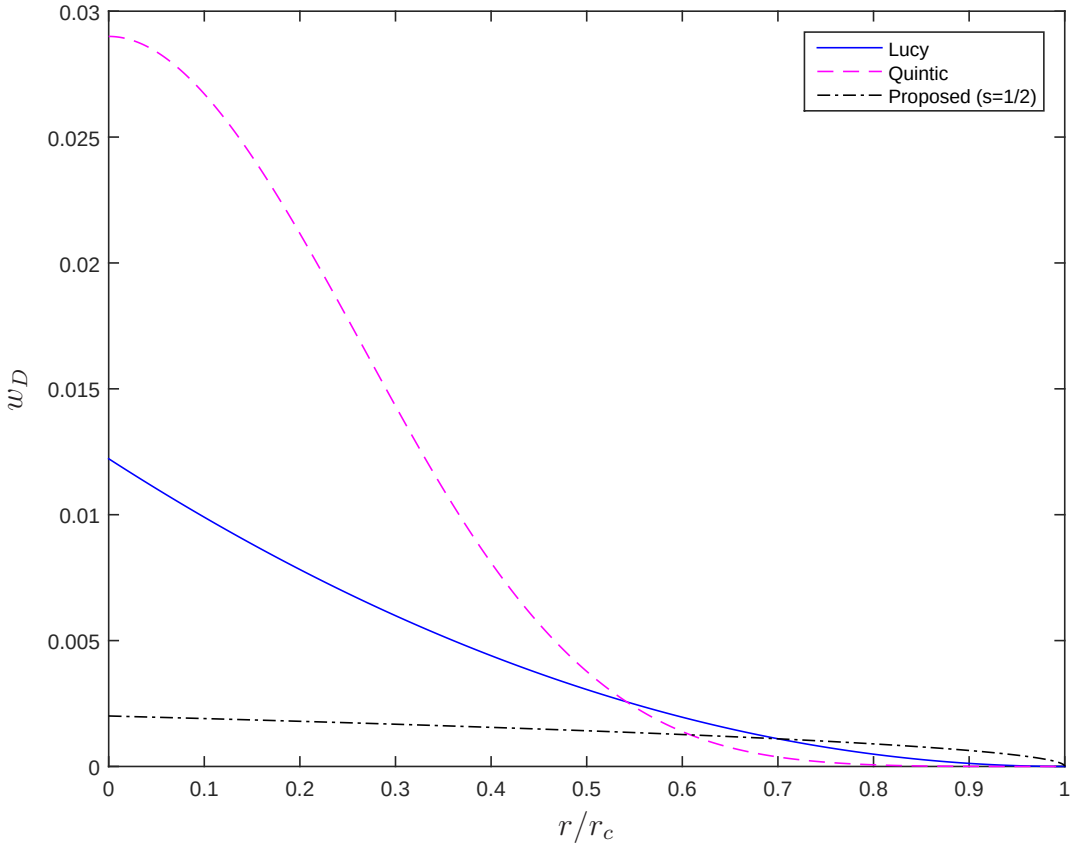

Figure 2: Variations of Lucy, quintic spline and proposed kernels (top) and their associated dissipative weighting functions (bottom) with $n = 4$ and $r_c = 2.5$.

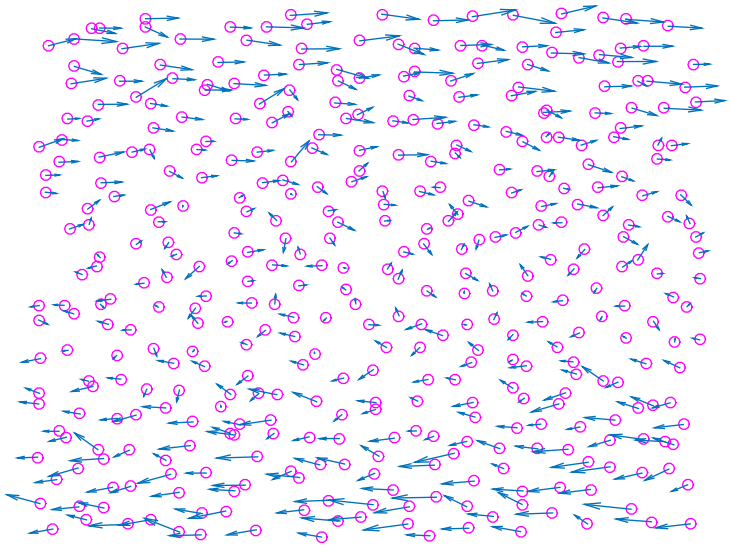

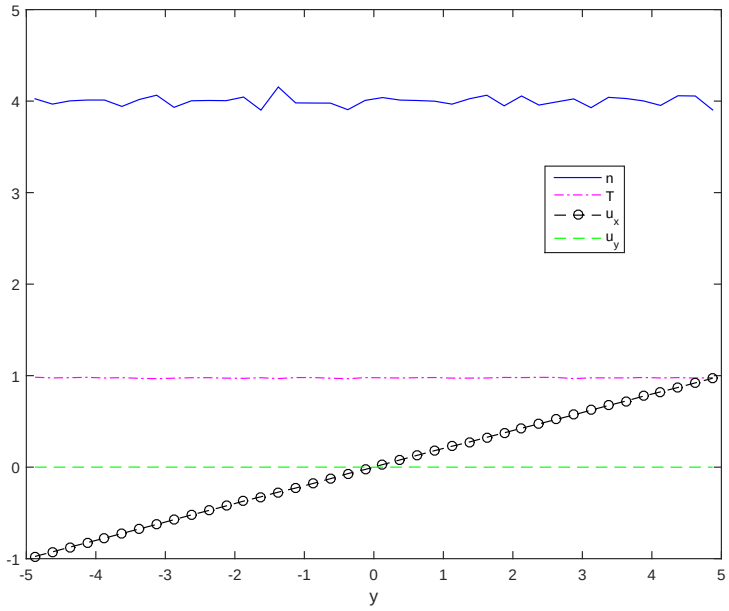

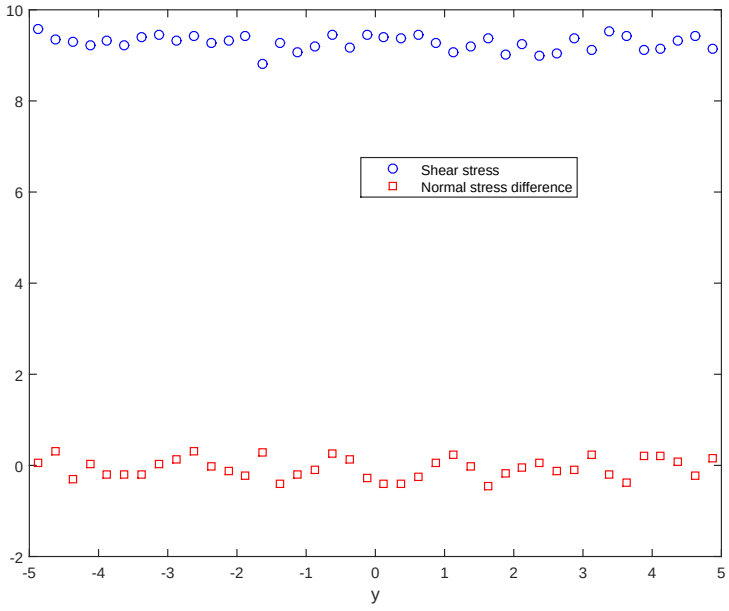

Figure 3: Couette flow, $m = 1, k_B T = 1, \eta_0 = 10$, shear rate of 1, 200000 time steps: results concerning spatial configuration at instant time and profiles of number density, Boltzmann temperature, normalised velocities and stresses on the cross section by the proposed DPD for the case of $r_c = 1$ and $n = 4$.

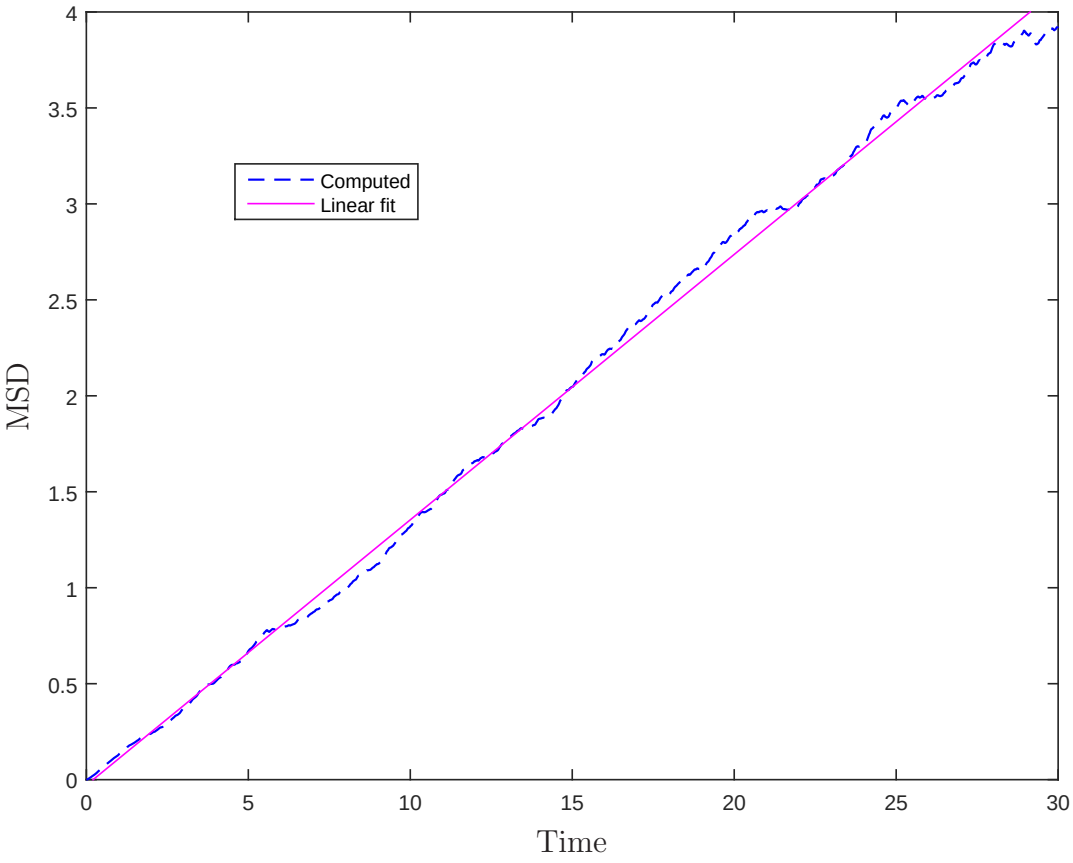

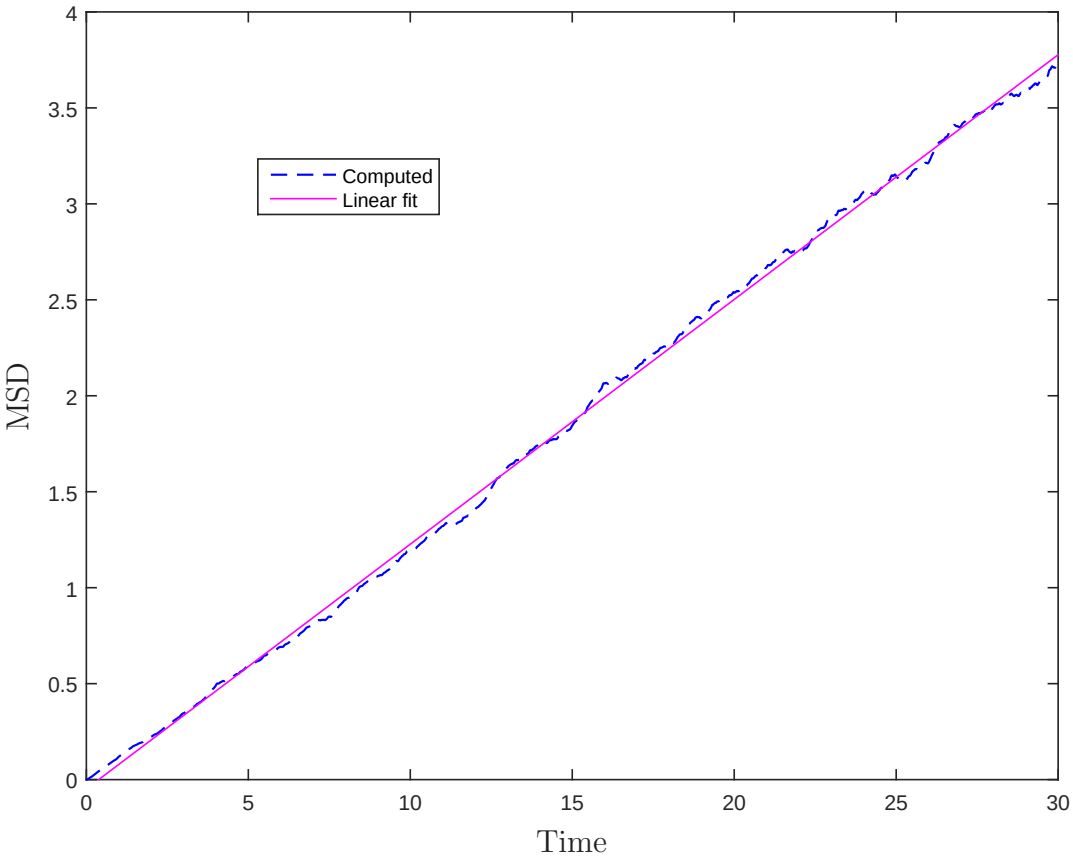

Figure 4: Proposed kernel, $m = 1, k_BT = 1, n = 4, r_c = 2.5, S_{c0} = 400, \eta_0 = 49$: the mean squared displacement (MSD) of the fluid particles against time by the proposed sDPD (top) and DPD (bottom). Linear fit results are included, from which the self-diffusion coefficients are estimated as 0.0346 for the proposed sDPD and 0.0319 for the proposed DPD which are comparable with the value of 0.0306 by the kinetic theory.

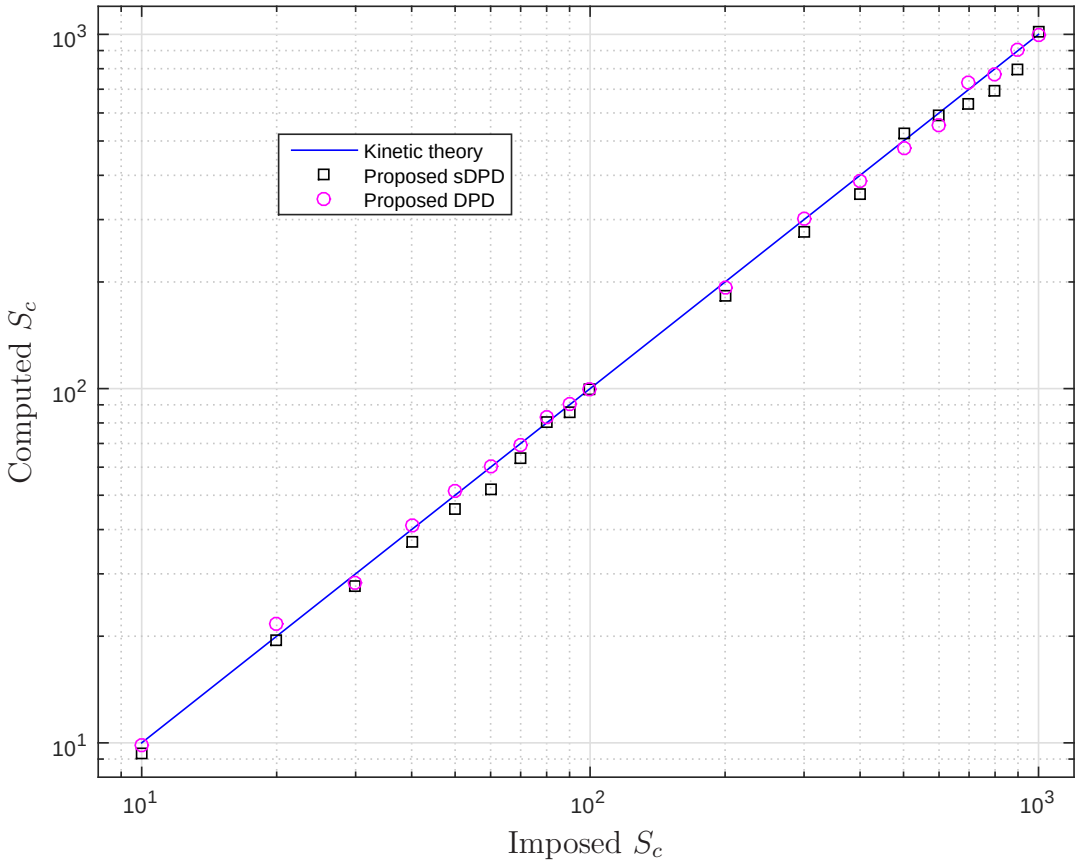

Figure 5: Proposed kernel, $m = 1, k_BT = 1, n = 4, r_c = 2.5$: Computed Schmidt numbers against the specified values, where the imposed viscosities are chosen to be integer values near their upper limits. Good agreement between the input and computed values is achieved. As designed, the kinetic theory predictions are exactly the same as the specified values. Results by the proposed DPD are generally closer to the specified values than those by the proposed sDPD. It is noted that the error-bars associated with the data points here are quite small and not displayed for visual clarity.